

A UNIVERSAL MODEL OF DROPLET VAPORIZATION APPLICABLE TO SUPERCRITICAL CONDITIONS

Zhou Ji*, Jiada Mo**
The University of Memphis
Memphis, TN

Alan S. Chow***
NASA/Marshall Space Flight Center
Huntsville, AL

K. X. He****
Alabama A&M University
Normal, AL

ABSTRACT

An evaporation model of a droplet has been constructed with the concern of the droplet under supercritical or near critical condition. The thermodynamic process involving liquid phase and gas phase as well as "blurred" state of the droplet around the critical point is integrated into a general framework. Thermodynamic properties and transport coefficients are modeled as functions of pressure, temperature and composition of the mixture. These functions and the equations of state are formulated over the range covering gas phase, liquid phase, and supercritical state. Numerical implementations of the model were made for an oxygen droplet in a hydrogen gas surrounding. Preliminary numerical results have demonstrated the feasibility of the concept even though further validation of the model is necessary when experimental data are available.

Nomenclature

n	molar concentration
X_1	molar fraction of species 1
m	mean molecular weight
u	radial velocity
T	temperature
p	pressure
h	enthalpy
J	mass flux
q	heat flux

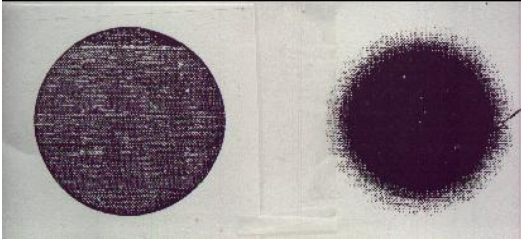
* Research Assistant
** Associate Professor, Mechanical Engineering
*** Aerospace Technologist
**** Assistant Professor, Physics

I. INTRODUCTION

Since the fuel oils are usually introduced into the combustors as sprays of droplets, it is reasonable to expect that the collective gasification of individual droplets would intimately influence the bulk spray vaporization and oxidation characteristics, which in turn determines the combustor performance. The droplet behavior is also considered as a major contributor to the spray combustion dynamics in liquid rockets, advanced gas turbines, and diesel engines. It has been suggested that it is irrelevant to study droplet combustion in that droplet vaporization, instead of combustion, is the dominant process during spray combustion. However, in many applications the vaporization happens at a very high pressure and temperature, which could probably be very close to or above the thermodynamic critical point. At the supercritical condition, the droplet or the environment can be in the state of neither liquid nor gas. The surface between the droplet and the environment does not exist any more. So no well-defined droplet is there. The primary question to be addressed, which is still kept open, is whether the droplets can reach criticality before they have been substantially gasified. This depends on the droplet gasification rate, droplet heating rate and the extent of elevation of the critical pressure due to dissolution of the ambient gas into the liquid. While the physics of criticality is an open question, any modeling taking the supercritical environment into account, or experimental techniques conducted under

supercritical conditions will be very helpful for further understanding the phenomenon.

The problem becomes significantly different when the pressure and temperature in the real chamber or the “flame chamber” are well above the thermodynamic critical states of the droplet liquid. It is possible that the droplet is heated up with its surface reaching the critical point prior to the end of the droplet lifetime. Then the sharp distinction between gas and the liquid disappears. The enthalpy of the vaporization reduces to zero, and no abrupt phase change is involved in the vaporization process. The density and temperature of the entire field of liquid droplet as well the ambient gases vary continuously across the droplet surface. The “droplet” itself does not exist in the usual sense. The different physical states can be depicted in figure 1. The word “droplet” can still be used to refer to a “blurred” region with high concentration of the original droplet species.



(a) subcritical (b) supercritical

Figure 1 Droplet surface blurred at supercritical condition

II. EQUATIONS OF MODELING

The system of fundamental equations include 1) Conservation Equations; 2) Transport Relations; 3) Equations of States and 4) Chemical Potential.

For the case of two species, molar concentration n is used instead of density, molar fraction instead of species density as unknowns in continuity equation, species equation, and the expressions of mass and heat fluxes.

The equation of mass, can be formulated in terms of n

$$\frac{n}{t} - \frac{1}{x} (nu) = \frac{n}{m} \frac{Dm}{Dt} - \frac{n}{m_i} m_j \frac{DX_j}{Dt}, \quad (1)$$

where the second equal sign is only to show an alternative form. m is the mean molecular weight.

The species equation becomes

$$\frac{DX_1}{Dt} - \frac{m}{mm_2} \bar{J}_1. \quad (2)$$

The energy equation is written as

$$C_p \frac{DT}{Dt} - vT \frac{Dp}{Dt} - \bar{q} - v m_1 \left(\frac{h_1}{m_1} - \frac{h_2}{m_2} \right) - \bar{J}_1 \quad (3)$$

The momentum equation is

$$-\left(\frac{u}{t} \right) - \frac{1}{x} \left(\frac{uu}{x} \right) - \frac{p}{x} - \frac{1}{x} \quad , \quad (4)$$

Equations (1), (2), (3), and (4) constitute the fundamental equations of a binary mixture fluid which is independent of the thermodynamic phase.

Transport relations and expression of chemical potential are used to develop the expressions for mass flux \bar{J}_1 and heat flux \bar{q} .

Denoting

$$\bar{J}_b = nD_m \left\{ D - X_1 \frac{m_1 m_2 X_1 X_2}{m} \left[\left(\frac{V_1}{m_1} - \frac{V_2}{m_2} \right) p - \left(\frac{h_2}{m_2} - \frac{h_1}{m_1} \right) \ln T \right] \right\} \quad (5)$$

we have

$$\bar{J}_1 = \frac{m_2}{m} (\bar{J}_b - X_1 X_2 k_T n D_m \ln T) \quad (6)$$

and

$$\bar{q} = (k_T RT) \bar{J}_b - k T \quad (7)$$

If we specify to the spherically symmetric case and spherical coordinates are used, as in a convection-free case, we can significantly simplify the foregoing fundamental equations further as follows, in which n , X_1 , u , T are the unknowns of the system.

$$-\frac{n}{t} - \frac{1}{r^2} \frac{1}{r} (nr^2 u) = \frac{n}{m} \left(-\frac{m}{t} - u \frac{m}{r} \right), \quad (8)$$

$$\left(-\frac{u}{t} - u \frac{u}{r} \right) - \frac{p}{r} - \frac{1}{r^2} \frac{1}{r} (r^2 p_r) = \quad (9)$$

$$\frac{X_1}{t} - u \frac{X_1}{r} = \frac{m}{mm_2} \frac{1}{r^2} \frac{1}{r} (r^2 J_1), \quad (10)$$

$$J_1 = \frac{m_2}{m} [J_b - X_1 (1 - X_1) k_T n D_m \frac{1}{T} \frac{T}{r}], \quad (11)$$

where

$$r = \frac{4}{3} \left(\frac{u}{r} - \frac{u}{r} \right), \quad (12)$$

$$v = \frac{4}{3} \left(\frac{u}{r} - \frac{u}{r} \right)^2, \quad (13)$$

$$J_1 = \frac{m_2}{m} [J_b - X_1 (1 - X_1) k_T n D_m \frac{1}{T} \frac{T}{r}], \quad (14)$$

$$q_r = (k_T RT) J_b - k \frac{T}{r}, \quad (15)$$

$$J_b = nD_m \left\{ D - \frac{X_1}{r} \frac{m_1 m_2 X_1 (1 - X_1)}{m} \right\} \quad (16)$$

$$\left[\left(\frac{V_1}{m_1} - \frac{V_2}{m_2} \right) \frac{p}{r} - \left(\frac{h_2}{m_2} - \frac{h_1}{m_1} \right) \frac{1}{T} \frac{T}{r} \right]$$

Also needed are the exact caloric equation of state, $h_i = h_i(V, T, X_i)$, and the thermal equation of state, $p = p(V, T, X_i)$ for the mathematical closure of

the system.

If the interface exists, there are 9 unknowns to be determined, i.e., u_b^L , u_b^G , R_d , X_{1b}^L , X_{1b}^G , T_b , p_b , \bar{v}_b^L , and \bar{v}_b^G on it. The extra unknowns come from the difference of u , X_1 , across the interface and the position of the interface in term of R_d . Correspondingly, the following relationships are needed to define them:

- 1) equation of state $p = p(\bar{v}, T)$
- 2) conservation of mass Eq. (8)
- 3) conservation of species Eq. (10)
- 4) conservation of momentum Eq. (9)
- 5) conservation of enthalpy Eq. (11)
- 6) evaporation law and surface heat flux,

$$q_b^G = q_b^L = L_b F_{ems}, \quad (17)$$

where mass emission flux F_{ems} is defined as

$$F_{ems} = \frac{1}{A_d} \frac{dm_d}{dt}. \quad (18)$$

where A_d is surface area of the droplet. F_{ems} needs to be determined from non-equilibrium thermodynamics.

- 7) the relation between mass emission flux F_{ems} and radius change rate $\frac{dR_d}{dt}$:

$$\frac{dR_d}{dt} = u_b^L - \frac{1}{\bar{v}_b^L} F_{ems}. \quad (19)$$

- 8) mass balance at the interface:

The mass balance can be expressed as

$(u_b^L \frac{dR_d}{dt}) - \bar{v}_b^L (u_b^G \frac{dR_d}{dt}) = \bar{v}_b^G F_{ems}$. After rearranging and using Eq. (19), it becomes

$$u_b^G - u_b^L = (\frac{\bar{v}_b^G}{\bar{v}_b^L} - 1) F_{ems}. \quad (20)$$

- 9) continuity of species flux, $\bar{J}_{1b}^G = \bar{J}_{1b}^L$.

III. IMPLEMENTATION AND NUMERICAL SCHEME

With the proper initial and boundary conditions, the system of equations (8) through (11) can be solved for unknowns X_1 , n , T , and u_r with the expressions of mass and heat fluxes in equations (14) to (16). Also needed are the following properties: mixture viscosity μ , heat conductivity of the mixture k , mutual diffusion D_m , the ratio of thermal diffusion to mutual diffusion k_T , and the following information related to the equations of state: thermal equation of state $V_i = V_i(p, T)$, caloric equation of state $h_i = h_i(p, T)$, $C_p(p, T) = (h/T)_{p, X}$, and $D(p, T) = 1 + X_i(\ln \bar{v}^i / X_i)_{T, p}$.

The equations of state in the present model are based on the Peng-Robinson equation of state

$$p = \frac{RT}{V - b} - \frac{a}{V(V + b)b(V - b)}, \quad (22)$$

$$\text{where } b = \frac{0.07780 RT_c}{P_c}, \quad a = \frac{0.45724 R^2 T_c^2}{P_c} [1 - f(1 - T_r^{1/2})]^2,$$

in which $f(\omega) = 0.37464 + 1.54226\omega - 0.26992\omega^2$ is a function of acentric factor ω . The subscript c indicates the critical properties. $T_r = T/T_c$ is reduced temperature.

Basically, the caloric equation of state for enthalpy for species i is expressed as

$$h_i = h_i^0 + h_i, \quad (23)$$

where h_i^0 is the reference enthalpy and h_i is the departure function. It is necessary to note that the enthalpy of a pure component is different from the molar partial enthalpy of a species in the mixture. The enthalpy of the mixture $h_m = \sum X_i h_i + H$, where h_i is enthalpy of pure component and H is the heat of mixing. In the current model, the heat of mixing is ignored, so that h_i is the same as molar partial enthalpy.

The result of curve fitting of the reference enthalpy for H_2 and O_2 is respectively

$$h_1^0 = RT(3.413 - 0.0193 \sqrt{p/p_{c1}}), \quad (24)$$

$$h_2^0 = RT(3.514 - 0.0136 \sqrt{p/p_{c2}}). \quad (25)$$

Generally the departure function can be obtained from pressure explicit equation of state using

$$h = \int^p \left(\frac{RT}{V} - T \left[\left(\frac{p}{T} \right)_V \right] \right) \frac{R}{V} dV - RT(Z - 1), \quad (26)$$

where $Z = pV/RT$. From the Peng-Robinson equation of state, it can be written as

$$h_i = \frac{1}{2\sqrt{2}b_i} \ln \frac{V_i - b_i + \sqrt{2}b_i}{V_i - b_i - \sqrt{2}b_i} \left(a_i - T \frac{a_i}{T} \right) \frac{RT}{p_i V_i} \quad (27)$$

The thermal equation of state is

$$V = V_{PR} - V_c + V_D, \quad (28)$$

where V_{PR} is molar partial volume in the Peng-Robinson equation of state as function of P , T and X_1 ; $V_c = \sum X_i V_{ci}$, in which

$$V_{ci} = V_{ci} + 0.3074 \frac{RT_{ci}}{P_{ci}},$$

is to give the proper compressibility factor Z_c for the pure limits;

$$V_D = \left(\frac{h^0}{p} - \frac{h^p}{p} \right)_{p, T_c}$$

gives effect of the calculated reference state, in which superscript p refers to perfect gas while 0 refers to actual reference state.

Using the Peng-Robinson equation of state (22), Eq. (28) is rearranged as pressure-explicit form

$$p = \frac{RT}{V - V_c - V_D - b} - \frac{a}{(V - V_c - V_D)^2 - 2b(V - V_c - V_D) + b^2} \quad (29)$$

Then it is necessary to evaluate the physical properties of the substances appearing in the fundamental equation. The pseudo-critical temperature T_{pc} and pressure p_{pc} are applied instead of true critical properties for the mixture, since the representations are much more simple while resulting in a considerable improvement of correlation. Pseudo-critical temperature is give by Kay as

$$T_{pc} = \sum X_i T_{ci} \quad (30)$$

Pseudo-critical pressure is calculated in this model with the modified Prausnitz-Gunn relation.

$$p_{pc} = \frac{RT_{pc} \sum X_i Z_{ci}}{\sum X_i V_{ci}} \quad (31)$$

where the critical compressibility factor may be estimated by using Kay-type relation.

$$Z_{cm} = \sum X_i Z_{ci} \quad (32)$$

At temperature of 0°C and pressure of 1 atm, the diffusivity of the H_2 - O_2 pair (gas) is $D_{12} = 0.697 \text{ cm}^2/\text{sec}$. This, in conjunction with a linear relation to temperature, is used in this model to determine diffusivity,

$$\frac{D_{m-m}}{T} = \text{constant} \quad (33)$$

where m is in centipoise, T is absolute temperature in °K, and D_{12} is in cm^2/sec .

An approximation of thermal-to-mutual $k_T = 0.3$ is used in the implementation of this model.

The viscosity of the mixture is also needed in this model. Although comprehensive research has been conducted and considerable data and formulas are available for viscosities of liquids and gases, little is known of the viscosity near critical condition. It is even more difficult for a mixture of multiple species. A relatively simple form of correlation is used in this model to calculate the viscosity of mixture, i.e.,

$$\mu_m = \frac{\sum X_i \mu_i(m_i)^{\frac{1}{2}}}{\sum X_i (m_i)^{\frac{1}{2}}} \quad (34)$$

The following equation, which was developed for a gas mixture, is chosen to evaluate thermal conductivity of mixture from individual component conductivity.

$$k_m = \frac{\sum X_i k_i (m_i)^{\frac{1}{3}}}{\sum X_i (m_i)^{\frac{1}{3}}} \quad (35)$$

Linear function fitting from tabulated experimental data is used to get conductivities for pure components H_2 and O_2 .

$$k_1 = 2.289 + 0.053T \quad (36)$$

$$k_2 = 0.043 + 0.009T \quad (37)$$

The coefficient D denotes the effect of non-ideality of the mixture, i.e.,

$$D = 1 - \sum X_i \frac{\ln \gamma_i}{X_i} - \sum \frac{\ln \gamma_i}{\ln X_i} - \sum \frac{\ln \gamma_i}{\ln X_i} \quad (38)$$

where γ_i is activity coefficient and f_i is fugacity coefficient.

With the Peng-Robinson equation plugged in,

$$D = 1 - \left\{ \frac{1}{(V - b)^2} (V^2 - \frac{b}{n_1}) - \frac{2}{RT (V^2 - 2bV - b^2)^2} \right. \\ \left. [(V - b)(V^2 - (V - b)\frac{b}{n_1}) - \frac{1}{n_1} \frac{1}{RT} \frac{1}{V^2 - 2bV - b^2}] \frac{X_1}{V} \left(\frac{m_1}{c_1} - \frac{0.29775 RT_{c1}}{p_{c1}} \right) \right\} \quad (39)$$

where

$$\frac{b}{n_1} = 0.07780 \frac{1}{n_1 Z_{c1} n_2 Z_{c2}} [V_{c1} (\frac{n_1 V_{c1}}{n_1 Z_{c1}} - \frac{n_2 V_{c2}}{n_2 Z_{c2}}) Z_{c1}]$$

$$0.07780 \frac{X_2 (V_{c1} Z_{c2} - V_{c2} Z_{c1})}{(X_1 Z_{c1} - X_2 Z_{c2})^2}$$

$$\frac{a}{n_1} = 0.45724 R [1 - f (1 - T_r)^{\frac{1}{2}}]^2 [(X_1 T_{c1} - X_2 T_{c2})$$

$$\frac{X_2 (V_{c1} Z_{c2} - V_{c2} Z_{c1})}{(X_1 Z_{c1} - X_2 Z_{c2})^2} - \frac{X_1 V_{c1} - X_2 V_{c2}}{X_1 Z_{c1} - X_2 Z_{c2}} \frac{X_2}{n} (T_{c1} - T_{c2})$$

Thermal expansion ratio is estimated with the formula of Smith et al. as

$$v = \frac{0.04314}{(T_c - T)^{0.641}} \quad (40)$$

where T_c will be replaced by the pseudo-critical temperature T_{pc} (66) of the mixture in the present model.

An acentric factor ω used in the Peng-Robinson equation of state is evaluated as

$$\log_{10} (X_1 P_{r1}^{sat} - X_2 P_{r2}^{sat})_{T_p} \approx 0.7 - 1.000 \quad (41)$$

where $p_r^{sat} = p^{sat} / p_c$ is reduced vapor pressure, $T_r = T / T_c$ is reduced temperature based on pseudo-critical temperature.

The model of constant-pressure heat

capacity C_p ($\frac{H}{T}$)_p is rarely accurate at high pressure. In the present model, it is calculated with the mixing rule of enthalpy h_m as

$$C_p = \left(\frac{h_m}{T}\right)_{p, X_1} = X_1 \frac{h_1}{T} + X_2 \frac{h_2}{T}, \quad (42)$$

the heat of mixture being ignored.

From equation (23), $\frac{h_i}{T} = \frac{h_i^0}{T} - \frac{h_i}{T}$. It is straightforward to get from (24) and (25) that

$$\frac{h_1^0}{T} = 3.413 R, \quad \frac{h_2^0}{T} = 3.514 R. \quad (43)$$

From Eq. (27),

$$\frac{h_i}{T} = \left[\frac{a_i}{V_i^2 - 2b_i V_i + b_i^2} X_i p \right] \frac{R}{RT (V_i^2 - 2b_i V_i + b_i^2)^2 - 2a_i (V_i - b_i)(V_i + b_i)^2}. \quad (44)$$

An explicit Mac-Cormack two-step predictor-corrector method is used as the basic numerical scheme. For equation (10) it is:

$$\text{Predictor step: } X_i^* = X_i^j + \Delta t^j; \quad (45)$$

$$\text{Corrector step: } X_i^{j+1} = \frac{1}{2}(X_i^* + X_i^j + X_i^*), \quad (46)$$

$$\text{where } X_i^j = \left[\frac{m_i^j}{n_i^j (m_2)_i^j} (J_1)_i^j \frac{X_{i-1}^j X_i^j}{r_{i-1} r_i} u_i^j \right] t^j, \quad (47)$$

$$X_i^* = \left[\frac{m_i^*}{n_i^* (m_2)_i^*} (J_1)_i^* \frac{X_{i-1}^* X_i^*}{r_{i-1} r_i} u_i^* \right] t^j. \quad (48)$$

For clarity, the original subscript "1" for species is dropped. Equations (8), (9) and (11) take similar formats.

The gradients of fluxes J_1 and q_r actually result in terms of second order derivatives of the primitive variables X_1 , p , T in the difference equations. In this implementation J_1 and q are evaluated using forward differences and the gradients calculated using backward difference, resulting in a central-difference scheme for those second-order derivatives. Take q as an example. From equations (15) and (16),

$$q_i = k_r RT_i (J_b)_i = k \frac{T_{i-1}}{r_{i-1}} - \frac{T_i}{r_i}, \quad (49)$$

where

$$(J_b)_i = n_i (D_m)_i \left\{ \left(\frac{X_{i-1}}{r_{i-1}} - \frac{X_i}{r_i} \right) \frac{1}{RT_i} - \frac{1}{m_i} \left[\left(\frac{m_2 X_2}{n} - \frac{m_1 X_1}{n} \right)_i \frac{p_{i-1}}{r_{i-1}} - \frac{p_i}{r_i} \right] \right. \\ \left. - (X_1 X_2)_i (m_1 h_2 - m_2 h_1)_i \frac{T_{i-1}}{r_{i-1}} - \frac{T_i}{r_i} \frac{1}{T_i} \right\}. \quad (50)$$

IV. RESULTS OF NUMERICAL EXPERIMENTS

The equation of state in this model is a modified Peng-Robinson equation of state. Fig. 2 show the result for pure hydrogen, the eleven curves, from bottom to top respectively, corresponding to the temperatures of 19.05, 21.89, 24.73, 27.57, 30.41, 33.25, 36.09, 38.93, 41.77, 44.61, and 47.45 °K. It is important for the model to be able to solve for the volume from the pressure and temperature too. As an example of other parameters, Fig. 3 exhibit the specific heat C_p a typical mixture ($X_1 = 0.5$).

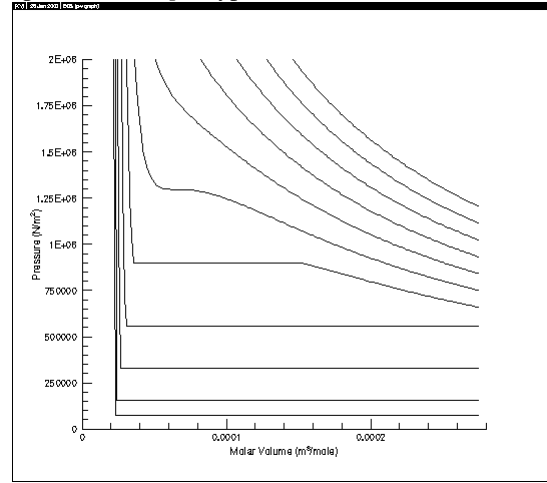


Figure 2 Peng-Robinson EOS for Hydrogen (48)

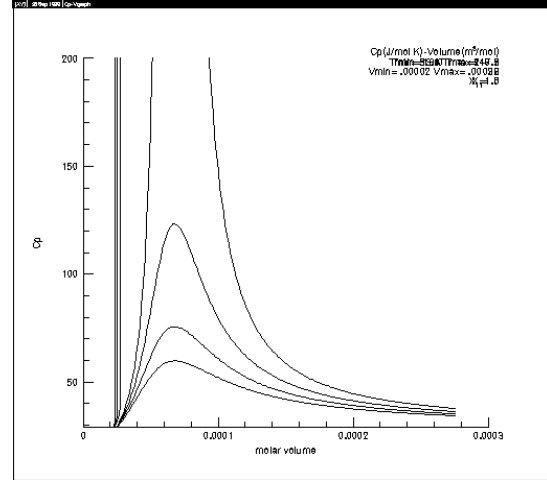


Figure 3 Cp of mixture, low temperature

The first numerical study presented here is the case beginning at an initial temperature of 200 K throughout the solution domain. Pressure is 1 atm. While pressure is low, the temperature is above the critical condition. At the initial instant, the spherical "droplet" region is occupied by pure oxygen. The outside surrounding is pure hydrogen. The oxygen sphere is actually in the gas phase, but there is a

discontinuity of density and concentration at the interface. See Fig. 4. Inside the interface, the density of oxygen is 1.957kg/m^3 . Outside the interface it is 0.1219kg/m^3 for hydrogen.

Fig. 5 shows that the initial distribution of temperature changes to a valley and peak pair around the original interface between two species at computational time step 2000. The corresponding physical time is $9.2 \cdot 10^{-5}$ seconds. From analysis of the actual computation procedure cases by the model, it is revealed that the major contribution of the temperature change comes from the term for the mass flux gradient in the energy equation. Though initially there are no gradients of temperature and pressure, the discontinuity of species concentration combined with the difference of unit mass enthalpy results in the change of the temperature, in spite of the fact that the molar enthalpies of the two sides are actually very close to each other. As time proceeds, the range of this valley-peak is stretched out. Fig. 6 shows the velocity distribution at the same time as in Fig. 5. The pattern of the valley-peak of velocity is more complicated than that of temperature, but it is quite obvious that these distortions are being smeared. Basically the results show that the mixture inside the interface moves globally toward the center, while outside the interface, the global velocity is outward. The result is not surprising after considering the fact that hydrogen, which has a lower density than oxygen, diffuses inwards. Fig. 7 presents the changed pressure. Although at the beginning, the pressure jumps because of the temperature discontinuity and the large gradient of concentration, the pressure tends to become uniform as the time proceeds. Fig. 8 is the concentration distribution. It is clear from this figure that the two species are undergoing mixing. Fig. 9 shows the density changes, which are calculated from the results of molar concentration of mixture and mean molecular weight.

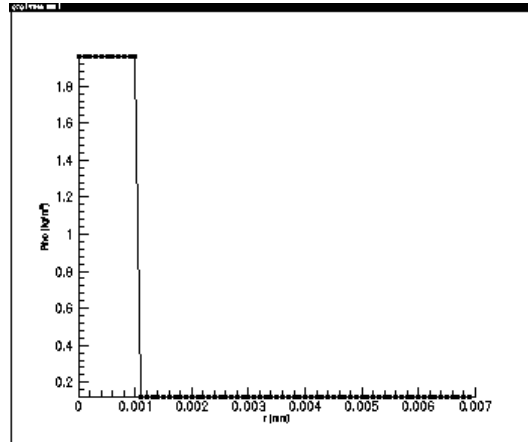


Figure 4 Initial Density

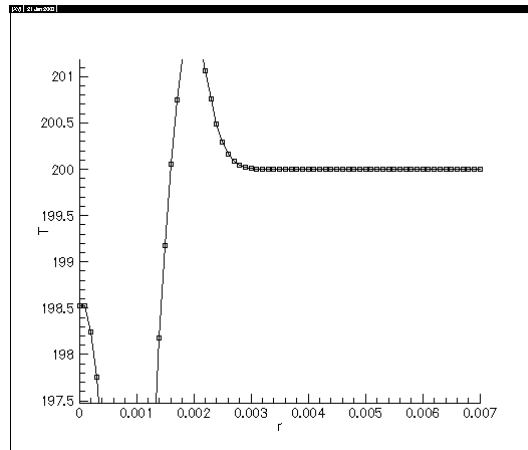


Figure 5 Temperature, 200 K, Step 2000

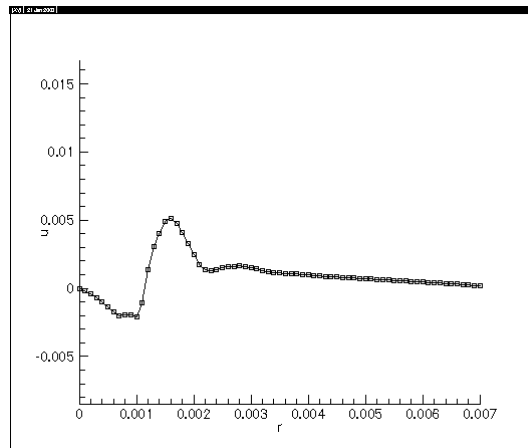


Figure 6 Velocity, Step 2000

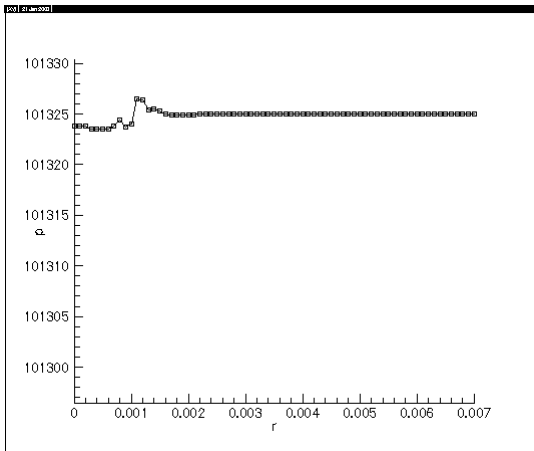


Figure 7 Pressure, Step 2000

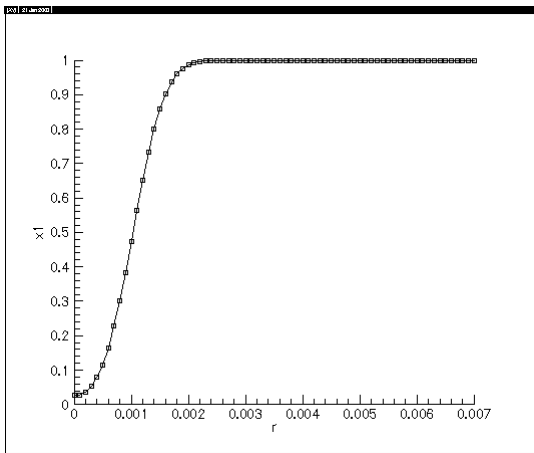


Figure 8 Species concentration, Step 2000

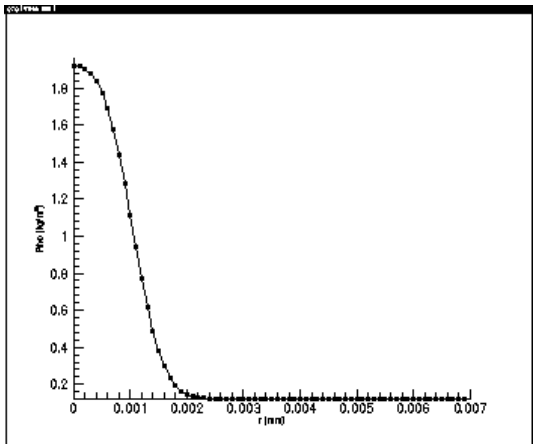


Figure 9 Density, Step 2000

Figs. 10 and 11 present the changing sequences of concentration and temperature distribution, respectively, in a photo type of simulated image. In Fig. 32 the white color represents hydrogen and black oxygen. The grayscale shows

concentration. In Fig. 33, the median gray stands for initial temperature and the lighter color shows higher temperature.



Figure 10 Species Concentration

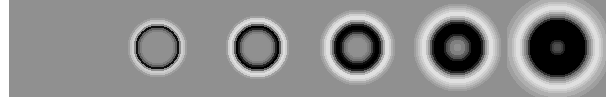


Figure 11 Temperature

Numerical results at higher pressure (10atm and 50atm) show that pressure has no significant direct influence on the temperature change near the interface. The velocity change is larger and the distribution of the species concentration and the density are almost the same as at 1 atm, except that density is proportionally larger.

When the droplet is in the liquid phase, the density difference across the interface is much larger than in the gas phase. Figs. 12, 13, and 14 show the modeling results with an initial temperature 91 K. This temperature is slightly above the boiling point of oxygen. The only difference between these results and the higher initial temperature case presented earlier, is that the temperature changes in a larger scale and the distribution curves are more complicated around the interface. As the initial temperature is lowered under oxygen's boiling point, the results become quite different. The temperature changes more drastically during the mass transportation process. The artificial viscosity has to be adjusted in the numerical scheme to get a stable solution. Figs. 15, 16, and 17 are the distributions of density, temperature and concentration at the time step 200 starting from an initial temperature of 90 K uniformly.

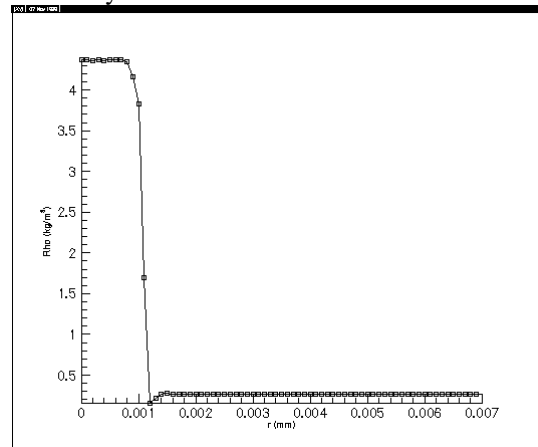


Figure 12 Density, 91K, step 500

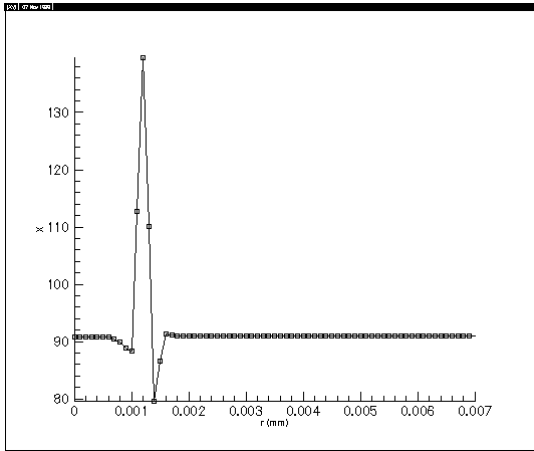


Figure 13 Temperature, 91K, step 500

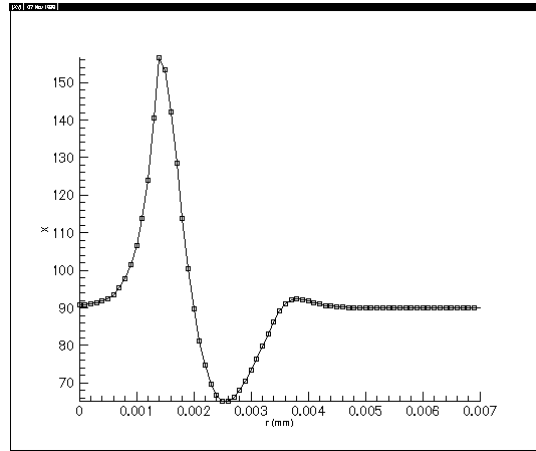


Figure 16 Temperature, 90K, step 200

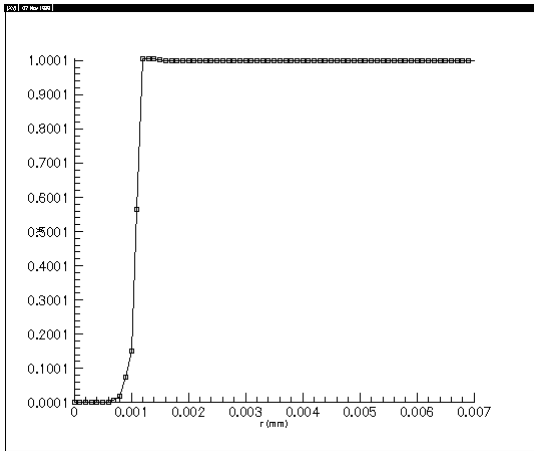


Figure 14 Concentration, 91K, step 500

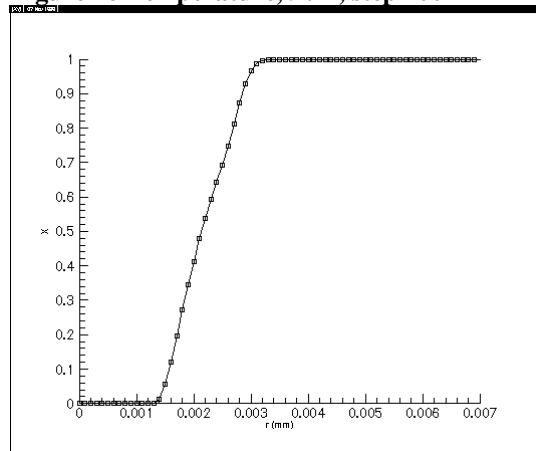


Figure 17 Concentration, 90K

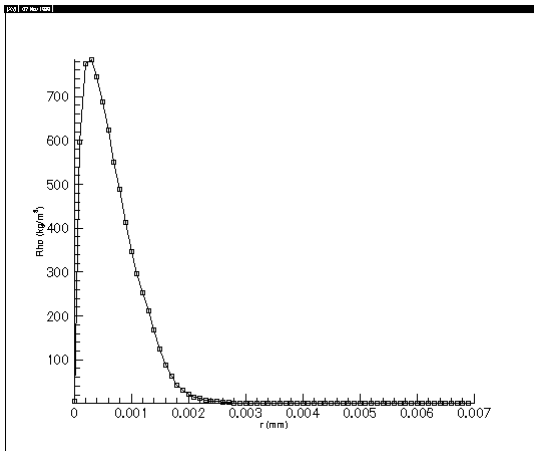


Figure 15 Density, 90K, step 200

What is most remarkable in the solutions is the qualitative difference between results for initial temperatures of 91 K and 90 K. The latter, is under the boiling point of oxygen, 90.15 K. The change of temperature around the interface is in opposite direction of all the gas cases. That change comes from the inward diffusion of hydrogen gas, whose enthalpy is much higher than that of liquid oxygen. In reality, the diffusivity in the liquid phase is much lower than that of gas, as mentioned before. The continuous model of diffusivity over the two phase ranges is too rough. The latent heat absorbed when liquid changes into gas also counteracts that trend of temperature change. The results imply that modeling diffusivity accurately and integrating latent heat in the caloric EOS are very important to make the present model complete. The density near the origin of the droplet is influenced strongly by the numerical oscillation, which is closely related to the numerical boundary condition there.

The interface treatment was not implemented in the above result for simplicity. So the whole process is dominated by diffusion. On the other hand, the difference between liquid and gas diffusivities is not modeled accurately enough. There is a difference of the order-of-magnitude in the diffusivities between the liquid and gas phase. Both problems are coupled to make the result of liquid droplet tentative. Nevertheless, the temperature distribution in the above results strongly suggests that the droplet could be heated up over the critical condition before it is completely vaporized.

As mentioned above, artificial viscosity is important in obtaining meaningful results. Other factors that could affect the numerical solutions include computational grid, time-step length, different methods to discretize pressure derivative, far-field solution conditions, and far-field boundary location. All the results presented here were obtained on a uniform grid of 310 points. Ten nodes of the grid are in the inner part ("droplet" region) and 300 nodes are in the outer region (surrounding). A finer grid and a corresponding smaller time step, a grid which is gradually stretched away from the droplet, and a smaller time step on the same grid have all been tested and they hardly make a noticeable changes in the results.

V. CONCLUSION

From the numerical findings of this study, the following conclusions can be drawn:

1) A universal model has been developed for droplet evaporation. Equations of states applicable to the supercritical condition have been identified. Actual equations of state of H_2 and O_2 are formulated and integrated into the model. Not only is this method applicable in the range of supercritical condition, but the specific phase is to be determined by the model itself too.

2) Thermodynamic properties are systematically modeled as function of pressure, temperature, and composition of H_2 - O_2 mixture. These models generally cover liquid, gas, and supercritical states in a universal form. The defect of previous model with constant or pre-determined properties is amended. Transport coefficients are modeled as functions of pressure, temperature and composition. Although the present result is to some extent only a conceptual one, it opens the possibility of generalization for study in this field.

3) Complete unsteady model is evaluated. All the deviations caused the pseudo-steady assumption are thus eliminated.

4) To make the model applicable for more general cases, forced and/or free convection in the surrounding of droplet, multicomponent fuel, existence of combustion, and effect of spray are some of the foreseeable factors that must be integrated in the model.

5) When interface dose exit, modeling the boundary conditions is still one of the major challenges.

Acknowledgements

The authors appreciate the financial support for this research provided by EEO office of NASA/MSFC, Mr. Williams Love is the Program Director.

REFERENCE

- [1] Bird, R. B., W. E. Stewart, E. N. Lightfoot, Transport Phenomena, John Wiley & Son, New York, 1960
- [2] Cussler, E. L., Diffusion: Mass Transfer in Fluid System, Cambridge University Press, 1992
- [3] Hanley, H. J., Transport Phenomena in Fluids, Marcel Dekker, 1969
- [4] Harstad, J., and J. Bellan, A Model of Critical and Supercritical Evaporation of Drops in Clusters, NASA Marshall Space Flight Center, 1993
- [5] Ji, Zhou, A Universal Model of Droplet Vaporization Applicable to Supercritical Conditions, Ph.D. Dissertation, The University of Memphis, 2000
- [6] Law, C. K., Recent Advances in Droplet Vaporization and Combustion, Prog. Energy Combust. Sci., Vol. 8., pp. 171-201, 1982
- [7] Perry, R. H., C. H. Chilton, Chemical Engineers' Handbook, 5th edition, 1973
- [8] Reid, R. C., J. M. Prausnitz, B. E. Poling, The Properties of Gas and Liquid, 4th edition, McGraw-Hill